JOURNAL OF Applied Polymer SCIENCE

The Effect of Selective Location of Carbon Nanotubes on Electrical Properties of Thermoplastic Vulcanizates

Yilei Zhu,[1,2] Xiaohong Zhang,[2] Zhihai Song,[2] Guicun Qi,[2] Xiang Wang,[2] Binghai Li,[2] Haosheng Wang,[1,2] Jinliang Qiao[1,2]

[1]College of Materials Science and Engineering, Beijing University of Chemical Technology, Beijing, China
[2]The Plastic Technology Center, Sinopec Beijing Research Institute of Chemical Industry, Beijing, China

Correspondence to: J. Qiao (E-mail: qiaojl.bjhy@sinopec.com)

ABSTRACT: Three types of conductive thermoplastic vulcanizates (TPVs) were prepared by blending polypropylene (PP), carbon nanotubes (CNT), and carboxylic acrylonitrile butadiene ultrafine full-vulcanized powdered rubber (xNBR-UFPR). The CNT locations were different in these three types of TPVs, i.e., CNTs were localized in PP matrix, in the xNBR-UFPR phase, or mainly in the interface. It had been found that TPV with CNTs localized mainly in the interface had the lowest conductive percolation threshold among these three types of TPVs. The volume resistivity of the TPV with 2 phr CNTs was as small as 220 Ω•cm. Moreover, the conductive TPV possessed good mechanical properties. © 2012 Wiley Periodicals, Inc. J. Appl. Polym. Sci. 000: 000–000, 2012

KEYWORDS: carbon nanotubes; conducting thermoplastic vulcanizates; polypropylene; xNBR-UFPR

Received 12 September 2011; accepted 14 March 2012; published online 00 Month 2012
DOI: 10.1002/app.37694

INTRODUCTION

Conductive elastomers have been the focus of considerable researches over the past two decades because of foreseeable applications in such diverse technologies as biological and chemical sensors, antistatic coatings, and electromagnetic interference shielding.[1,2] Among different conductive elastomers, conductive thermoplastic vulcanizate (TPV) has been found the most promising one due to its low-conductive percolation threshold on account of volume exclusion effect.

For the conductive composites with binary-polymer blends, the selective localization of conductive fillers played a key role in the composites' electrical properties because of different efficiency of conductive pathway formed by conductive fillers.[2] In TPV with conductive fillers, there are three types of morphologies: (1) the fillers are localized in the dispersed rubber phase, (2) in the plastic matrix, or (3) in the interface between plastic matrix and rubber particles. For traditional conductive TPV, the conductive fillers can be dispersed only in the rubber phase via the dynamic vulcanization process or in the plastic matrix via the two-step process.[3,4] However, it is very difficult to control the location of conductive fillers in conductive TPVs via the dynamic vulcanization process.[5–8] Moreover, the effect of the location of fillers is very important for the properties of TPV, especially for the electrical property.[9,10]

To compare the electrical properties of TPVs with three types of morphologies, the conductive TPV with fillers localized in the different locations had to be prepared first. Our previous articles reported a series of rubber particles with ca. 100 nm in diameter named ultrafine full-vulcanized powdered rubber (UFPR), which could be used to prepare TPV.[11,12] The location of fillers in such TPV was decided by the particular combination of polymer and UFPR. It was attributed to the varied interaction between fillers and polymer (or UFPR).[13–16]

This article will report the effect of location of carbon nanotubes (CNT) on electrical and mechanical properties of TPV. Conductive TPVs with three types of morphologies were prepared by blending polypropylene (PP), CNTs, and carboxylic acrylonitrile butadiene ultrafine full-vulcanized powdered rubber (xNBR-UFPR). CNTs were localized in PP matrix, in the disperse phase (xNBR-UFPR) or in the interfaces, respectively. The ideal morphology for the conductive TPV was found in this study, which had to be helpful for designing high-performance conductive elastomers.

EXPERIMENTAL SECTION

Materials

The multiwalled-carbons nanotubes (CNT) were FloTubes™ 9000 (CNano Technology, Beijing) whose purity was more than

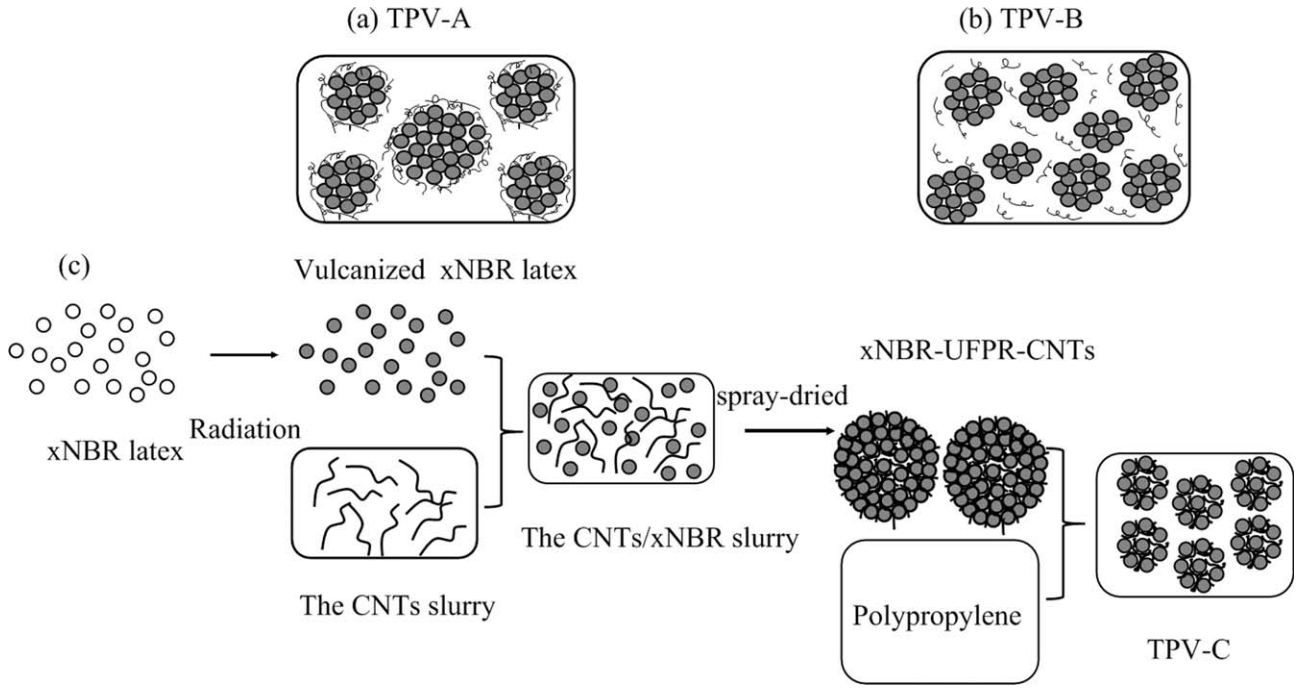

Figure 1. Schematic illustration for the morphology of TPV-A (a), TPV-B (b), and preparation process of TPV-C (c). The solid black circle represents the xNBR-UFPR, and the black line corresponds to CNT.

95%. Their average diameter was ca. 11 nm and their average length was ca. 10 μm. The surface area was 230–250 m^2/g. The CNTs slurry was the LB™ 200, which was the composites of CNTs (FloTubes™ 9000), dispersant, and water. The CNT and dispersant loading were 5 and 0.2 wt%, respectively. The CNT used in the slurry were unfunctionalized.

Isotactic PP was grade 0# (China Blue-Star Petrochemical, Tianjing). Their melt index was 0.9 g/10 min (230°C, 2.16 kg).

The maleic anhydride grafted polypropylene (PP-*g*-MA) was Bonp® GPM 200AL (Nengzhiguang New Materials Technology, NingBo). The grafted ratio of maleic anhydride was 0.9% and the melt index was 40 g/10 min (230°C, 2.16 kg).

The acrylonitrile butadiene latex premixed with a certain amount of multifunctional monomer was irradiated by gamma rays and then xNBR-UFPR (Narpow™ VP501) was obtained by spray drying of the crosslinked rubber latex, according to the patent technology.[17]

Sample Preparation

TPV-A with CNTs localized in the interfaces as shown in Figure 1(a) was prepared by blending PP, xNBR-UFPR, and CNTs simultaneously in an internal mixer (Brabender PLE 651) at 210°C with 70 rpm for 10 min. The weight ratio of xNBR-UFPR/PP was 70/30. Before the melt blending, three components were premixed via the high-speed mixer. TPV-B with CNTs dispersed in PP matrix as shown in Figure 1(b) was prepared by blending PP-*g*-MA, xNBR-UFPR, and CNT simultaneously at the same condition and same weight ratio of xNBR-UFPR/PP of TPV-A. The preparation process of TPV-C with CNTs dispersed in UFPR phase was illustrated in Figure 1 (c). First, the CNT slurry was added dropwise into irradiated rubber latex and the compound latex was then stirred for 60 min to form uniform mixture. Then, rubber particles with CNTs, named xNBR-CNTs, were obtained after spray-drying. The weight ratio of CNTs to rubber varied from 1/70 to 1/10. Finally, TPV-C was prepared via blending PP-*g*-MA and xNBR-CNT powders simultaneously in an internal mixer (Brabender PLE 651) at 210°C with 70 rpm for 10 min. The weight ratio of xNBR-CNT powders to PP-*g*-MA varied from 71/30 to 77/30.

Testing and Characterization

Electrical Resistivity. Plates with diameter100 mm and thickness 2 mm were prepared by melt-compression at 200°C for 7 min with 10 kN and were subsequently cool-compressed at 25°C for 3 min with 5 kN. For the measurement of resistivity above $10^7\Omega$ cm, the plates were measured using a PC68 Digital Teraohmmeter (Shanghai Precision & Scientific Instrument) according to the ASTM D257-2007. For the measurement of resistivity below $10^7\Omega$ cm, the strips cut from the plate were measured by four-point test fixture combined with a Resistivity Tester (Gibitre Instruments) according to the ASTM D991.

Morphology Observation. The morphologies of the conductive TPVs were observed using transmission electron microscope (TEM, Philips TECNAI 20) at 200 keV. Ultrathin sections of 100 nm in thickness were cut using a glass knife at −60°C with a cut angle of 45° and collected on 400 mesh copper grids. Then, these ultrathin sections were stained by osmium tetroxide before observation.

Mechanical Properties. Tensile tests were carried out on a tensile testing machine (SHIMADZU AG-1, Japan) according to ASTM D412-06a. The adopted speed of the crosshead was

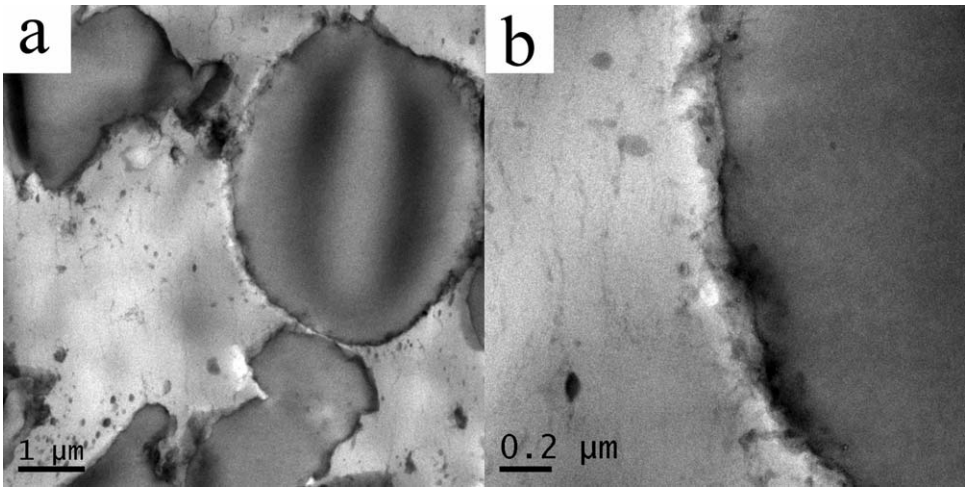

Figure 2. The TEM micrographs of TPV-A with 1 phr CNTs. The weight ratio of xNBR-UFPR/PP was 70/30.

500 mm/min. Compression set was measured at room temperature for 22 h according to ASTM D395-03.

RESULTS AND DISCUSSION

Morphology of the Three Types of TPVs

The three types of TPV were prepared via blending PP (or PP-*g*-MA), CNT, and xNBR-UFPR (or xNBR-CNT powder). TEM images of TPV-A, TPV-B, and TPV-C with 1 phr CNTs are shown in Figures 2, 4, and 5, where the continuous phase is PP or PP-*g*-MA matrix, the dispersed phase is rubber, and the hollow tube is CNT.

The surface-loading structure with the xNBR-UFPR acting as carriers of CNT was formed in TPV-A with low CNT loading during the premixing process.[14] The interaction between xNBR-UFPR and CNT was stronger than that between PP and CNT during the blending process. It was very difficult for CNTs to migrate from the surface of xNBR-UFPR into PP matrix or rubber phase. Therefore, CNTs in TPV-A could only be localized in the interface as shown in Figure 2. A few of CNTs could not be absorbed on the xNBR-UFPR surface as the increase of CNTs. Therefore, these CNT would be dispersed in PP matrix. The higher the CNT loading, the more CNTs in PP matrix. When the CNTs loading was high, CNTs were observed not only in the interface of two polymer but also in PP matrix as shown in Figure 3.

The matrix was PP-*g*-MA instead of PP in TPV-B, which resulted in that all of CNTs were localized in matrix as shown in Figure 4. This morphology of TPV might be attributed to two reasons: surface energy and melt viscosity. First, surface energy of the unfunctionalized CNT was much higher than that of PP.[18] PP-*g*-MA had much higher surface energy, which can reduce the interfacial energy between CNT and PP-*g*-MA; second, the melting index of PP-*g*-MA [40 g/10 min (230°C, 2.16 kg)] was much higher than that of PP [0.9 g/10 min (230°C, 2.16 kg)], which indicated that the melt viscosity of PP-*g*-MA was lower than that of PP. The particles normally tend to be preferentially incorporated into the lower viscosity polymer.[19]

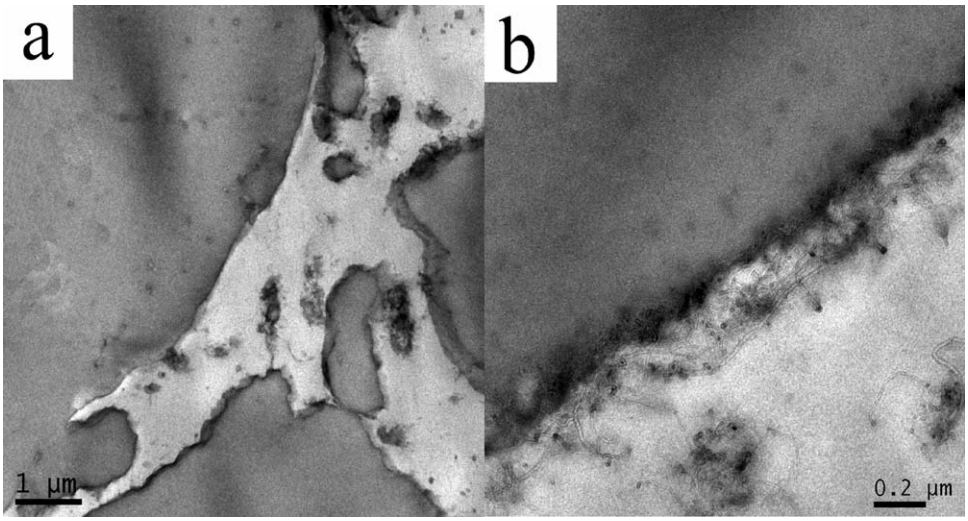

Figure 3. The TEM micrographs of TPV-A with 2 phr CNTs. The weight ratio of xNBR-UFPR/PP was 70/30.

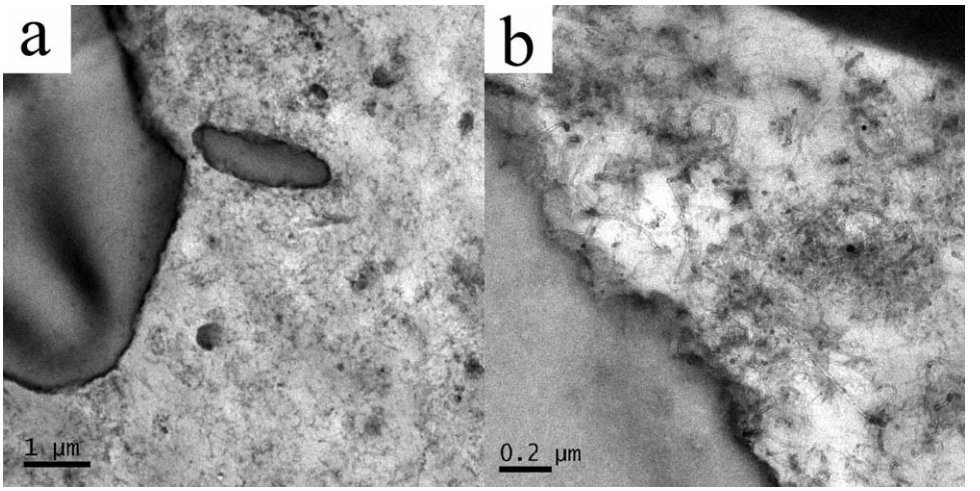

Figure 4. The TEM micrographs of TPV-B with 1 phr CNTs. The weight ratio of xNBR-UFPR/PP was 70/30.

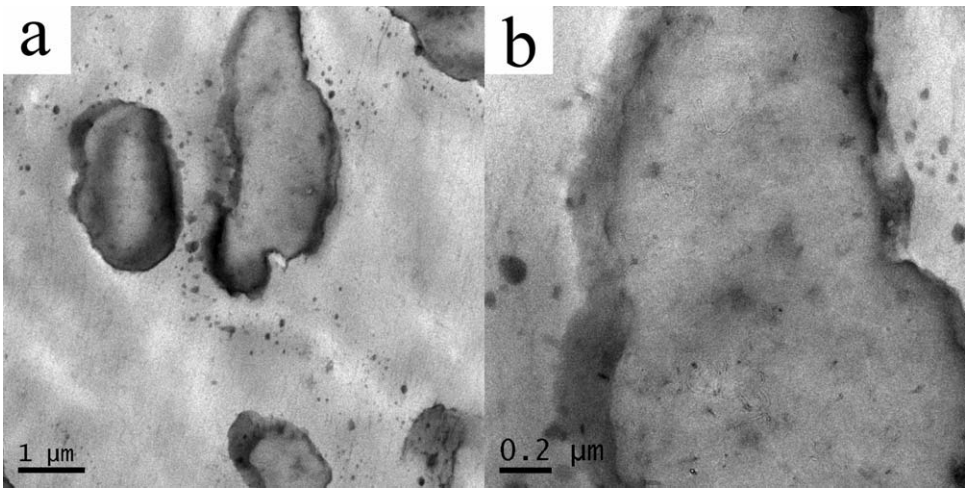

Figure 5. The TEM micrographs of TPV-C with 1 phr CNTs. The weight ratio of xNBR-UFPR/PP was 70/30.

Therefore, CNT could be stayed in PP-*g*-MA matrix as shown in Figure 4.

CNTs and UFPRs interpenetrated each other in TPV-C because of the special process mentioned in section "Sample Preparation" as shown in Figure 1. During the blending process, the xNBR-CNTs powders could not be dispersed individually during the blending process, which was attributed to the poor interaction between the PP matrix and the rubber particles; therefore, CNTs could be stayed only in the rubber phase as shown in Figure 5.

The Electrical Properties of the Three Types of TPVs

The effects of the CNT loading on the volume resistivity of the three types of TPVs were shown in Figure 6. As expected, the volume resistivity depends not only on the CNTs loading but also on the location of CNTs. The percolation threshold of TPV-A, TPV-B, and TPV-C were 1.5, 2, and 4 phr, respectively. Above the percolation threshold, the volume resistivity reached a plateau and the value could be reduce to 50 Ω•cm when the CNTs loading was 7 phr for TPV-A and TPV-B.

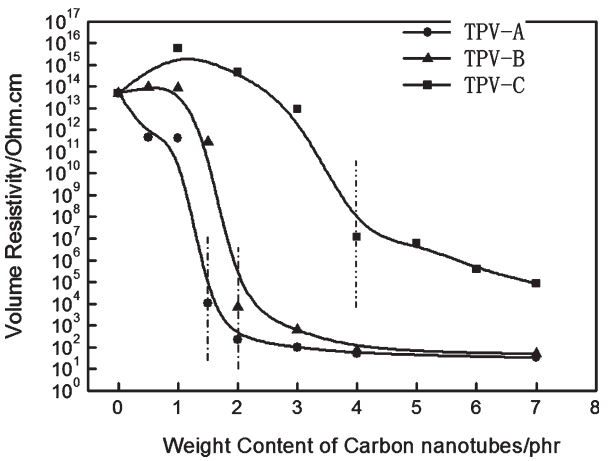

Figure 6. The volume resistivity of TPV (-A, -B, and -C) as a function of CNTs loading. The weight ratio of xNBR-UFPR/PP was 70/30 in these three types of TPVs.

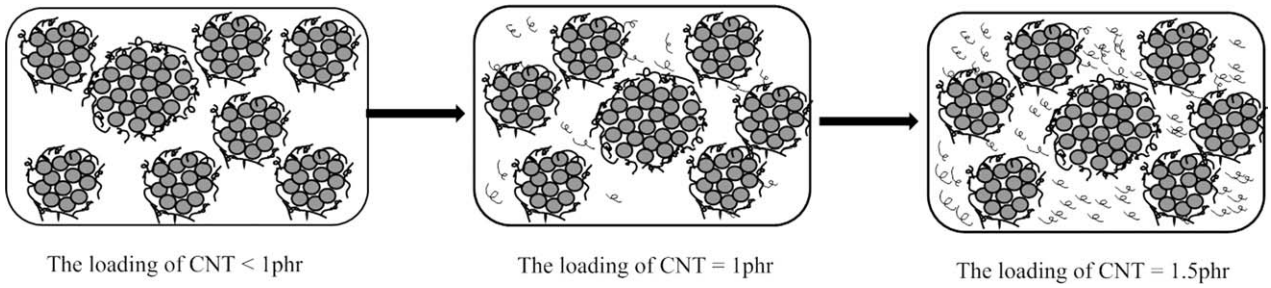

Figure 7. Schematic illustration of the approaching the percolation threshold.

Table I. Mechanical Properties of TPV- (A, B, and C)

CNT loading/phr		0	1	2	3	4	7
TPV-A	Tensile strength/MPa	5.91	5.83	6.41	7.04	7.88	9.21
	Compression set/%	40	41	43	47	48	49
TPV-B	Tensile strength/MPa	6.02	-	7.81	-	-	-
	Compression set/%	38	-	40	-	-	-
TPV-C	Tensile strength/MPa	5.91	-	6.67	-	-	-
	Compression set/%	40	-	44	-	-	-

The percolation threshold of TPV-C was the highest and that of TPV-A was the lowest among three types of TPVs. Why is TPV-A the best one in conductivity? CNTs were chosen first to be localized in the interface in TPV-A, then CNTs had to be dispersed into PP matrix when most of rubber particles had been covered. As shown in Figure 3, when CNTs loading reached 2 phr, a certain amount of CNTs were dispersed in PP matrix, which could connect conductive rubber particles to form an effective conductive pathway.

To sum up, the formation of conductive pathway of TPV-A was illustrated schematically in Figure 7. CNTs preferred to be localized in the interface of binary polymer phases and formed a conductive-shell covering xNBR-UFPR particles when CNT loading was low (<1 phr CNT). Some CNTs could be dispersed in PP matrix as the increase of CNTs loading (>1 phr CNT). When CNT loading was up to the percolation threshold (1.5 phr CNT), a majority of xNBR-UFPR particles, covered with the conductive CNTs, could be connected by the CNTs in PP matrix. Therefore, such morphology is the most effective one for conductive TPV with conductive filler.

The Mechanical Properties of the Three Types of TPVs

The tensile strength and compression set of TPV-(A, B, and C) were given in Table I. The tensile strength were improved as the increasing of CNT loading in TPV-A. The tensile strength of TPV-B was the best and the tensile strength of TPV-A and C were comparable when CNT loading was 2 phr. This result was attributed to the selective location of CNTs in TPV. CNTs could enhance the strength of PP matrix and further improve the tensile strength of TPV-B if CNTs only located in matrix. As for compression set, the values increased slightly after the incorporation of CNTs. However, electrically conductive TPV-(A, B, and C) still possessed good compression set.

CONCLUSION

Three types of conductive CNTs/xNBR-UFPR/PP TPVs were prepared by traditional-melt blending instead of dynamic vulcanization. CNT could be controlled to be localized in PP matrix, in the dispersed phase of xNBR-UFPR or mainly in the interface, respectively. An ideal morphology for the conductive TPV has been found, i.e., most of CNTs were localized in the interface to form a conductive shell covered the rubber particle and a few of CNTs were dispersed in PP matrix as bridges to connect the conductive rubber particles to form conductive pathway. The conductive TPV with such ideal morphology had a very low-conductive percolation threshold and conductive TPV with volume resistivity of 220 Ω•cm could be prepared when CNT loading was only 2 phr. Moreover, the conductive TPV possessed good mechanical properties.

ACKNOWLEDGMENTS

This research was subsidized by the Special Funds for Major State Basic Research Projects (2005CB623805).

REFERENCE

1. Ailish, O. H.; Fergal, O. M.; Peter, M. J. *Appl. Phys.*, **2008,** *104*, 1.
2. Al-Saleh, M. H.; Sundararaj, U. *Carbon,* **2009,** *47*, 2.
3. Katbab, A. A., Nazockdast H., and Bazgir S., *J. Appl. Polym. Sci.,* **2000,** *75*, 1127.
4. Tian, H.; Tian, M.; Zou, H.; Dang, Z.; Zhang, L. J. *Appl. Polym. Sci.*, **2010,** *117*, 691.
5. Baudouin, A.-C.; Autl, D.; Tao, F. F.; Devaux, J.; Bailly, C. *Polymer* **2011,** *52*, 149.
6. Goldel, A.; Kasaliwal, G.; Potschke, P. *Macromol. Rapid. Commun.*, **2009,** *30*, 423.

7. Wu, D.; Lin, D.; Zhang, J.; Zhou, W.; Zhang, M.; Zhang, Y.; Wang, D.; Lin, B. *Macromol. Chem. Phys.,* **2011,** *212*, 613.
8. Wu, D.; Sun, Y.; Lin, D.; Zhou, W. Zhang, M.; Yuan, L. *Macromol. Chem. Phys.* **2011,** *212*, 1700.
9. Gubbels, F.; Blacher, S.; Vanlathem, E.; Jerome, R.; Deltour, R.; Brouers, F.; Teyssie, Ph. *Macromolecules,* **1995,** *28*, 1559.
10. Feng, J. Y.; Chan, C. M.; Li, J. X. *Polym. Eng. Sci.,* **2003,** *43*, 1058.
11. Zhang, X. H.; Wei, G. S.; Liu, Y. Q.; Gao, J. M.; Zhu, Y. C.; Song, Z. H.; Huang, F.; Zhang, M. L.; Qiao, J. L. *Macromol. Symp.,* **2003,** *193*, 261.
12. Xu, X. D., Qiao, J. L., Yin, J. H. *J. Polym. Sci. B.* **2004,** *42*, 1042.
13. Xinqing, S.; Jinliang, Q.; Youqing, H.; Yiqun, L.; Xiaohong, Z.; Jianming, G.; Banghui, T.; Zhihai, S. *Acta Polym. Sin.,* **2005,** *1*, 142.
14. Wang, H. S.; Zhang, X. H.; Zhu, Y. L.; Song, Z. H.; Qiao, J. L. *Mater. Lett.* **2011,** *65*, 2055.
15. Gui, H.; Zhang, X.; Dong, W.; Wang, Q.; Gao, J.; Song, Z.; Lai, J.; Liu, Y.; Huang, F.; Qiao, J. *Polymer* **2007,** *48*, 2537.
16. Wang, H. S.; Zhang, X. H.; Zhu, Y. L.; Song, Z. H.; Qiao, J. L. *Chin. J. Polym. Sci.,* **2012,** *30*, 138.
17. Qiao, J.; Wei, G.; Zhang, X.; Zhang, S.; Gao, J.; Zhang, W.; Liu, Y.; Li, J.; Zhang, F.; Zhai, R.; Shao, J.; Yan, K.; Yin, H. *US Patent US 6,423,760 B1*, **2002.**
18. Barber, A. H.; Cohen, S. R.; Wagner, H. D. *Phys. Rev. Lett.* **2004,** *92*, 1.
19. Fenouillot, F.; Cassagnau, P.; Majeste, J.-C. *Polymer* **2009,** *50*, 1333.